ANALOGIES BETWEEN SIMPLE MECHANICAL SYSTEMS AND ELECTROHYDRAULIC AND ELECTROMECHANICAL SERVOMECHANISM

Parid Alimhillaj*   Edmondo Minisci**   Matteo D.L. DallaVedova***   Altin Dorri****

*, **** Energy Department, Faculty of Mechanical Engineering, Polytechnic University of Tirana

** University of Strathclyde, Glasgow G1 1XJ, United Kingdom

*** Politecnico di Torino, Turin 10129, Italy

ABSTRACT

Contemporary flight control system design necessitates the use of intricate models to analyse individual components or subsystems. However, fundamental and synthetic models with sufficient accuracy are essential for preliminary design, monitoring, or diagnostic purposes. Understanding primary flight commands, particularly those represented as position servo commands with a high degree of accuracy, is greatly enhanced through analogies drawn between simple mechanical systems and electrohydraulic as well as electromechanical servomechanisms. By employing these analogies, complex systems can be simulated using simpler yet still accurate models. In this study, we present methods of simplification aimed at simulating electrohydraulic and electromechanical servomechanisms using a second-order dynamic system with two degrees of freedom. This approach preserves the desired accuracy in the simulation while comparing favourably with results obtained from more complex validated mathematical models in MATLAB/Simulink.

Keywords: Flight control systems, MATLAB/Simulink, second order dynamic system, mathematical model.

1 INTRODUCTION

Seeking to highlight the analogy existing between the electro-hydraulic systems or electromechanical ones, representable by a simple second-order model. Firstly, we examine the system (depicted in Fig. 1) consists of a mass M moving along the x-axis on a horizontal plane (in the absence of friction) [8-9]. The motion is influenced by the combined action of an external force F, elastic forces generated by two ideal springs with stiffness Kass and Krel, and damping forces from a viscous damper with dimensional damping coefficients Cass and Crel. The elastic and viscous forces associated with Krel and Crel are due to the relative motion existing between the mass M and the movable surface (moving along an independent coordinate y, lying on the same axis as x).

Contact author: Parid Alimhillaj1

Polytechnic University of Tirana, Sheshi "Nene Tereza", Nr. 4, Tirana, Albania.
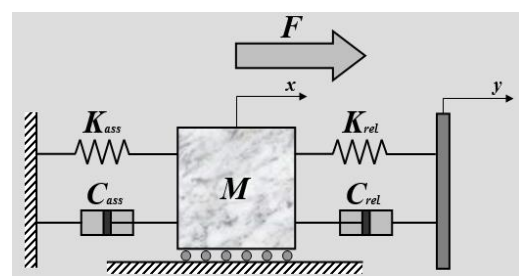E-mail: parid.alimhillaj@fim.edu.al

Figure 1 Schematic representation of the physical system under examination.

In this case using the schematic representation provided in Fig 2, one can easily derive the equation of equilibrium for the forces acting on the mass M in Fig 1. In the analogy with a flight control servo, the movable surface is represented by mass M, while the movable wall y, which in its motion relative to x produces a force proportional to the relative displacement x-y (through an ideal stiffness spring of stiffness K_{rel}) and a force proportional to the relative velocity (through a viscous damper with dimensional damping coefficient C_{rel}), simulates the control stick.
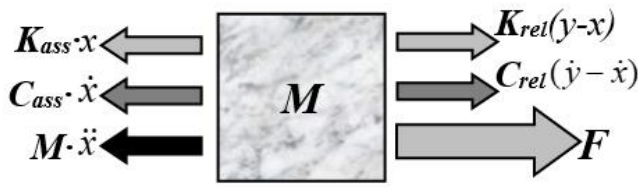
Figure 2 Schematic representation of the force equilibrium along the x-axis.

Relative or absolute stiffness and damping simulate different characteristics of the servo mechanism:

- K_{rel}: simulates the control action, proportional to the relative position error, produced by the proportional component (GAP) of the servo mechanism controller. This stiffness can be interpreted as the proportional position loop gain, as it produces a force on the movable surface proportional to the instantaneous position difference measured between the command input from the stick (input y) and the position of the movable surface (output x).

- C_{rel}: provides a force contribution proportional to the relative velocity between the movable surface (i.e., the mass translating with velocity dx/dt) and the stick (i.e., the movable wall having velocity dy/dt), thus reasonably simulating the possible derivative contribution (GAD) of the servo mechanism control logic.

- K_{ass}: simulates the effect of the aerodynamic field on the movable surface (i.e., the aerodynamic force arising on the movable surface when it, moved by the system, moves from the zero aerodynamic position). For the model to correctly simulate a servo mechanism, it is necessary that $K_{ass} \ll K_{rel}$.

- C_{ass}: simulates the fluid dynamic damping inherent in the servo mechanism structure (particularly fluid leaks through orifices and valve clearances) and the contribution due to a possible velocity loop (GAS) (which, unlike GAD gain, contributes to the regulation proportionally only to the velocity of actuation of the movable surface) and, in the case of electromechanical servo mechanisms, also to the counter electromotive force (CEMF)

At every moment, the force F is balanced by the algebraic sum of the inertia force M·d²x/dt², the elastic forces of the two springs, and the damping forces produced by the two dampers. Bringing all the unknown terms to the left side of the equation, and the known terms to the right side, we obtain the following expression:

$$M\frac{d^2x}{dt^2} + (C_{ass} + C_{rel})\frac{dx}{dt} + (K_{ass} + K_{rel})x = F + C_{rel}\frac{dy}{dt} + K_{rel}y \qquad (1)$$

The equation 1 can be written as follow:

$$\frac{d^2x}{dt^2} = \frac{1}{M}\left\{ \bar{\xi} - (C_{ass} + C_{rel})\frac{dx}{dt} - (K_{ass} + K_{rel})x \right\} \qquad (2)$$

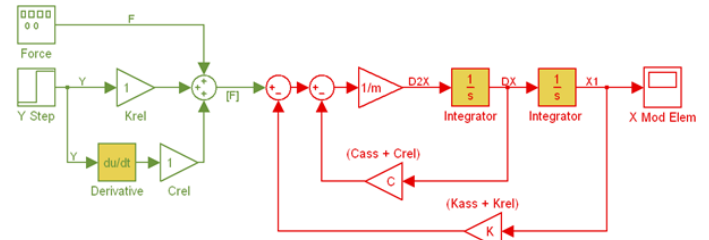The "elementary" block diagram of equation 2 is: [4-5]:

Figure 3 Block diagram created using elementary MATLAB/Simulink blocks.

2 GENERAL CONSIDERATIONS AND MATHEMATICAL MODEL

The block diagram of the complete electrohydraulic servomechanism as explain in [1-3, 14] is:
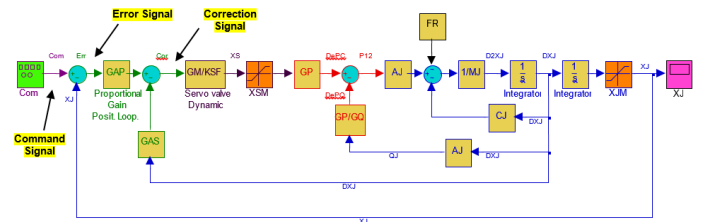

Figure 4 Block diagram of the electro-hydraulic position servomechanism.

In concluding the conceptual part of the system modeling, we can compare the structure of the electro-hydraulic servomechanism model in Fig. 4 with the block diagram obtained by examining the electromechanical servo system reproduced in Fig. 5 referred to [9].
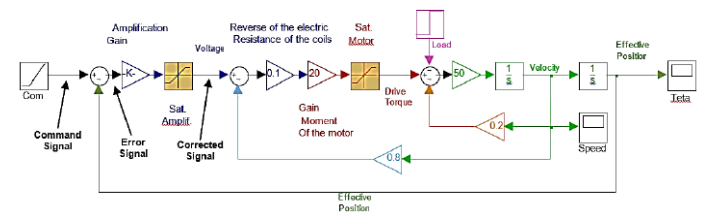

Figure 5 Block diagram of the electro-mechanic position servomechanism.

The structures of the models are nearly identical; in both cases, we can identify subsystems that perform analogous tasks:

- Electronic components that, by comparing command signals with feedback signals, process control currents through control logic.

- A subsystem that convert and amplifies the correction signal to enable subsequent signal transformation (the amplifier and the electromechanical model of the servo valve).

- A subsystem that converts the correction signal into the corresponding power signal (electric motor and fluid dynamic model of the servo valve).

- Mechanical transmission (assumed to be infinitely rigid and free of mechanical clearance) that, by transferring the power signal to an actuator, produces the movement of the controlled aerodynamic surface and the transducers that close the feedback loops.

For these considerations, the further analysis and results are referred to the electrohydraulic servomechanism, as they are specular for the electromechanical one [10-13].

2.1 MATHEMATICAL MODEL

Highlighting the analogy between the electro-hydraulic system, represented by the simple second-order model discussed above (Fig. 4), and the two-input mass-spring-damper system (whose characteristics have already been illustrated in Fig. 3), it is appropriate to reformulate the corresponding block diagram as follows. [2-4]
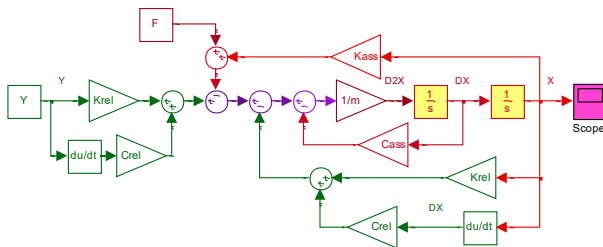

Figure 6 Block diagram created using elementary MATLAB/Simulink blocks elaborating the Figure 3.

It is immediately evident how the parallelism between relative stiffness and relative damping coefficient (derivative) repeats twice in the block diagram (i.e., downstream of the forcing function Y and in the position feedback loop). It is appropriate to consider relocating the closure of the position feedback loop (which gives its influence both through Krel and, via the derivative dY/dt, through Crel) upstream. This is done to consolidate identical blocks, as indicated by the repetition of the parallelism between relative stiffness and relative damping coefficient in both downstream sections, namely after the forcing function Y and within the position feedback loop.
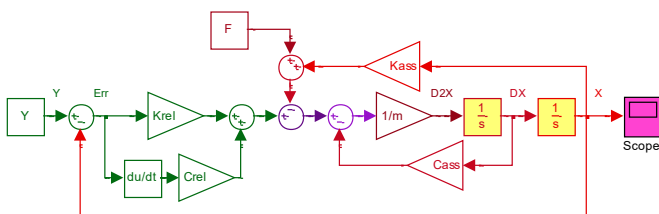

Figure 7 Block diagram two-input mass-spring-damper system, reformulated according to Fig. 1 with the relative modifications

The latest formulation of the block diagram can also be derived directly by explicitly expressing the term in the maximum derivative in eq. (3) rather than in (1), as done to obtain the formulation in Fig. 3 after several steps. [6-7]

$$M \frac{d^2 x}{dt^2} + C_{ass} \frac{dx}{dt} + K_{ass} x + C_{rel}(\frac{dx}{dt} - \frac{dy}{dt}) + K_{rel}(x - y) = F \qquad (3)$$

It is worth noting that the mentioned analogy is only possible if the model represented by the block diagram in Figure 4 is rearranged according to the formulation in Figure 7, linearized by eliminating the saturation block that represents the limit switch of the valve spool. This is modified by introducing two additional terms, one of which accounts for the possible presence of a derivative term GAD in the control, parallel with the proportional position gain GAP (remembering that this is present only as an alternative to the velocity feedback loop), and the other expresses the possible component of the aerodynamic load proportional to the deflection of the movable surface XJ, according to the proportionality constant Kass. The complete functional equivalence between the two-input mass-spring-damper system and the electro-hydraulic system can be established by assigning specific values to the coefficients of the mass-spring-damper, as determined by the following relationships:

$$C_{ass} = CJ + \frac{GP}{GQ} AJ^2 + GAS \frac{GM}{KSF} GP \cdot AJ =$$
$$= CJ + \left(\frac{AJ}{GQ} + GAS \frac{GM}{KSF}\right) GP \cdot AJ \qquad (4)$$

$$K_{ass} = K_{aer} \qquad (5)$$

$$C_{rel} = GAD \frac{GM}{KSF} GP \cdot AJ \qquad (6)$$

$$K_{rel} = GAP \frac{GM}{KSF} GP \cdot AJ \qquad (7)$$

$$M = MJ \qquad (8)$$

In comparing Figures 7 and 4, the following observations emerge:

- The equivalent of "Cass" in Figure 7 is depicted in Figure 4 through various actions and reactions that articulate the connection between the absolute velocity DXJ and the corresponding force components acting on the actuator (including damping contributions, gain loop effects, and velocity loop ones).
- The equivalent of "Crel" in Figure 7 finds representation in Figure 4 through various actions and reactions that elucidate the relationship between the relative velocity dErr/dt and the corresponding force acting on the actuator (involving contributions from the derivative of the control logic).
- The equivalent of "Krel" in Figure 7 is illustrated in Figure 4 by diverse actions and reactions that convey the association between the relative position Err and the corresponding force acting on the actuator (encompassing the proportional position contribution of the control logic).
- The same effect to "M" in Figure 7 is reflected in Figure 4 by the presence of MJ.
- The equivalent of "Kass" in Figure 7 is portrayed in Figure 4 by Kaer.

The same considerations can be applied to the Electro-Mechanical Servomechanism (SMEM) by assigning the coefficients of the mass-spring-dumper system values obtained from the SMEM data shown in the block diagram of Figure 8 using the following relationships:

$$M = MJ$$

$$Kass = Kaer \tag{9}$$

$$Crel = GAD \cdot \frac{GM}{R} \tag{10}$$

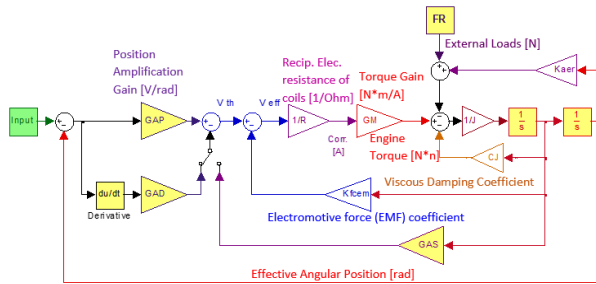Figure 8 Simulink model of the analysed SMEM.

$$Krel = GAP \cdot \frac{GM}{R}$$

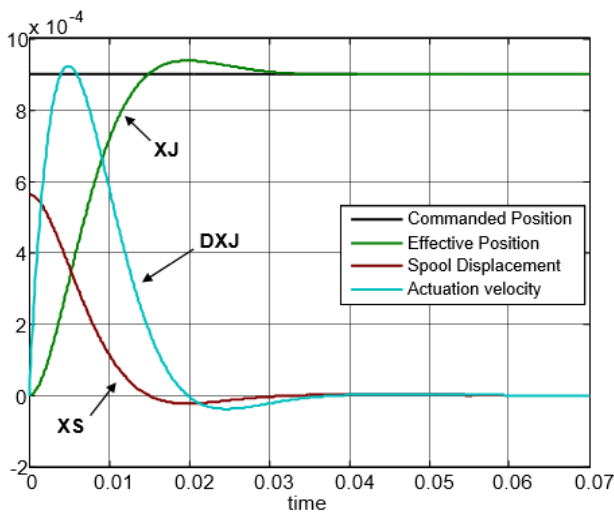$$Cass = (Kfcem + GAS) \cdot \frac{GM}{R} + CJ \tag{11}$$

Figure 9 Dynamic response of the electrohydraulic servomechanism block diagram scheme to a step command ComC = 0.0009 [m].

3   RESULTS OF THE SIMULATION

In Figure 9, is presented the response generated by an electrohydraulic servomechanism, where is depicted a step command with an amplitude of ComC = 0.0009 m. At the initial instant of the simulation, the controlled surface is at position XJ = 0, while the commanded position instantly shifts from zero to ComC. Consequently, the position error, represented by the algebraic sum ComC - XJ and initially zero, undergoes a step increase.
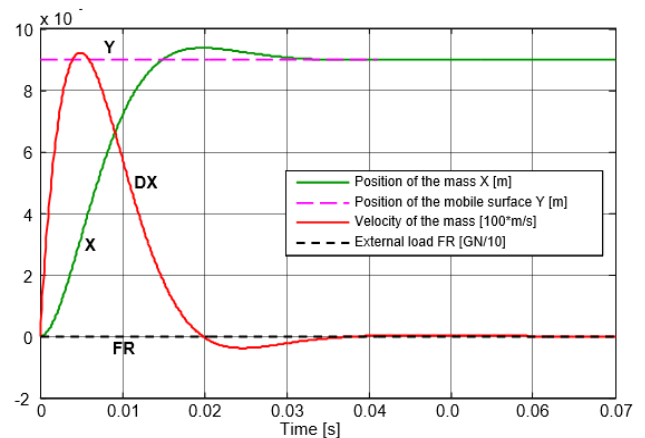

Figure 10 Response of the mass-spring-dumper with step input Y = 0.0009 [m] in the case of Krel = 50 [MN/m], Crel = 0 [Ns/m], Cass = 320050 [Ns/m].
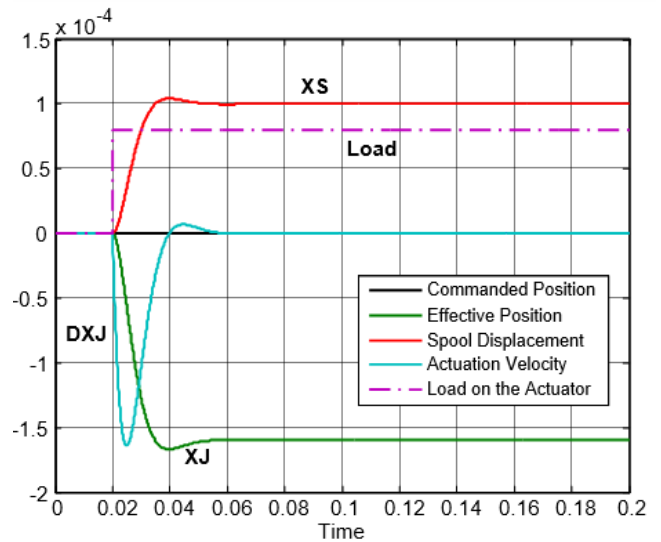

Figure 11 Electrohydraulic servomechanism response to an external load FR = 8000 [N] without command.

The position error is processed by the system, resulting in a response that manifests as the initiation of a pilot current to the valve, leading to an immediate displacement of the spool XS (without reaching its end position, i.e., without saturation intervention) and the generation of differential pressure and driving force (produced by the hydraulic actuator). Under the action of this force, the initially stationary system moves and progressively accelerates, developing an actuation velocity DXJ and moving towards ComC with the aim of reducing the position error. Naturally, as the position error decreases, the accelerating action produced by the hydraulic actuator diminishes, while the decelerating action linked to damping effects increases with the growing velocity. At the moment the servo mechanism reaches the commanded position, the error is nullified. However, if the actuation velocity remains positive, overshoots may occur. As soon as overshoot is triggered, the error changes sign and begins to increase (in magnitude) as the actual position deviates from the commanded one.

The system responds by producing a torque to stop the piston and then reversing its motion to bring position error back to zero. Depending on the system's stability, piston area, gains of the adopted amplifier and valve, and simulated damping conditions (underdamped, overdamped, or critically damped system), very different responses can be obtained, characterized by stable response dynamics. In the other side, if we see the Fig. 10, of mass-spring-dumper system, the similarities with the electrohydraulic servomechanism behaviour are pretty the same, despite that the mass-spring-dumper is simpler in its block diagram construction. In Figure 11, the illustration depicts the system's response to the application of an external load FR. In the context of linear actuators, we will specifically discuss external loads, while in the case of rotary actuators, we will focus on torques generated by forces or external loads. The servo mechanism, initially at rest, perceptively recognizes the external load FR as a force capable of inducing backward movement. This triggers the generation of a position error, Err, to counteract the applied load. This is achieved through the subsequent opening of the spool represented by XS, leading to the development of a corresponding differential pressure. As it can be seen the two graphics presented in Figure 11 and Fig. 12, which represents the behaviour of the system under external loads are perfectly identic, despite some minor changes, as example in Fig. 11 is simulated the spool displacement as well, but it is not simulated in mass-spring-dumper system in Fig. 12, as well as some other minor discrepancies in transitory phase. In Fig. 13 is presented the case of a ramp command with a slope ComR = 0.1 [m/s] applied to the Electrohydraulic Servomechanism with an increased GAP set to 105 [mA/m], in a system scenario in which no derivative or velocity loop is active. As in the previous cases the response of the mass-spring-dumper system (Fig. 14) is identical to the electrohydraulic servomechanism (Fig. 13) with some minor discrepancies, as the presence of spool displacement line in the electrohydraulic servomechanism simulation.
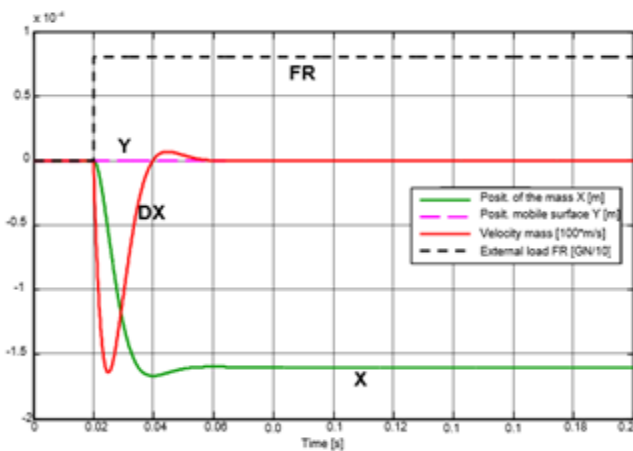
The case depicted in Figure 15, presents the response of the electrohydraulic servomechanism to a step command which is designed not to trigger the intervention of the saturation block related to the limit switch of the valve spool (XSM). Additionally, there is a load proportional to the actual position of the actuator according to the constant Kass. These modifications result in the servo mechanism's inability to reach the commanded position (due to the load caused by Kass*XJ, which leads to a residual position error) and the persistence of oscillations typical of an increased proportional gain GAP without either derivative control or a velocity loop control.
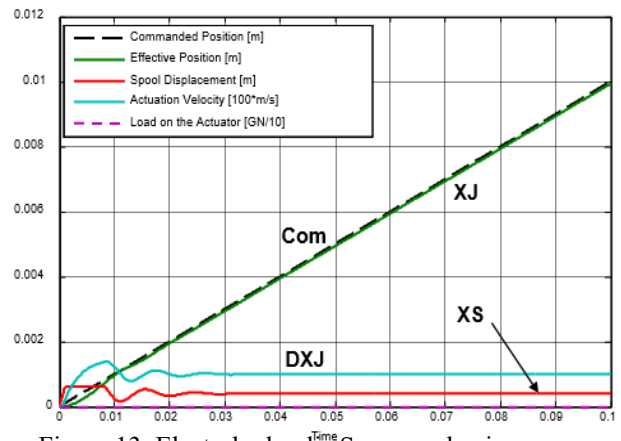

Figure 13 Electrohydraulic Servomechanism response to a ramp command ComR = 0.1 [m/s] with position gain increased to GAP = 105 [mA/m] and derivative gain GAD = 0 [mA*s/m].
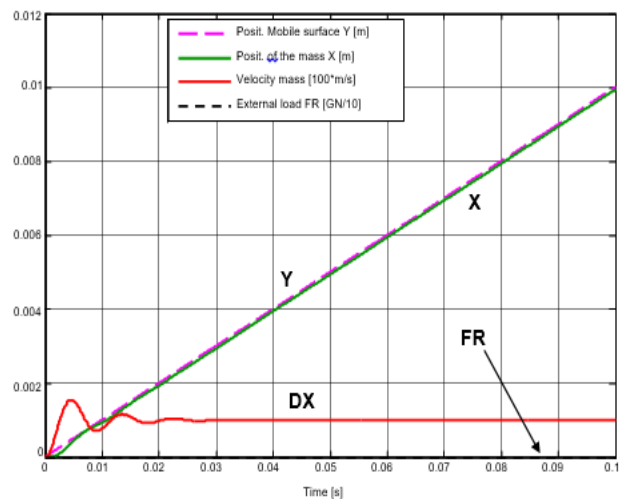

Figure 14 Dynamic response of the mass-spring-dumper system to a ramp command with a slope ComR = 0.1 [m/s] with increased relative stiffness Krel = 500 [MN/m], Kass = 0 [N/m], Crel = 0 [Ns/m], and Cass = 320050 [Ns/m].

Figure 12 Response to an external load F = 8000 [N], with input Y = 0 [m], in the case of Krel = 50 [MN/m], Crel = 0 [Ns/m], and Cass = 320050 [Ns/m].
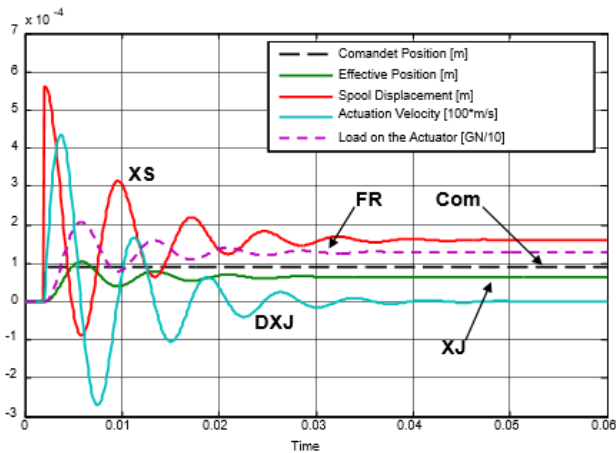
Figure 15 Electrohydraulic Servomechanism response to a small step command ComC = 910-5 [m] with a load proportional to the displacement, Kass = 2108 [N/m], and an increased proportional gain (GAP).

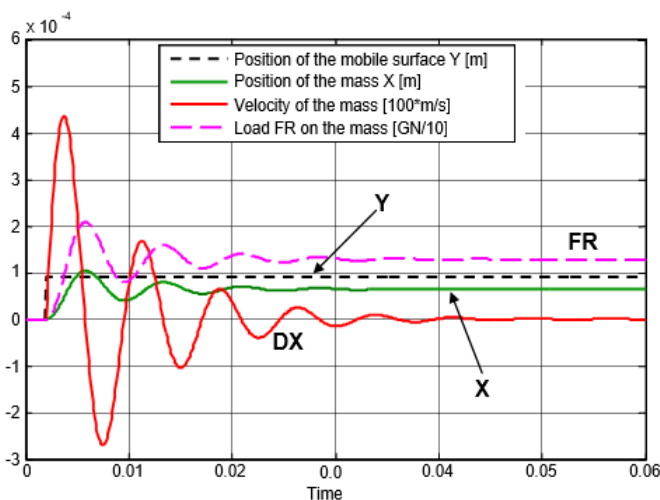

Figure 16 Response of the mass-spring-dumper system to a step input $Y = 9 * 10^{-5}$ [m] of the mobile frame, increased Krel = 500 [MN/m], Crel = 0 [Ns/m], Cass = 320050 [Ns/m], and Kass = 200 [MN/m].

In Fig. 16, is presented the same identical case as in Fig. 15 but run on the mass-spring-dumper model, as it can be seen the two figures are identical, with some minor discrepancies mostly related that in the Electrohydraulic servomechanism simulation it is added the actuation velocity line, which is missing in the mass-spring-dumper simulation.

4 CONCLUSION

From the simulation graphs in Figs. 10, 12, 14 and 16, when compared to the corresponding simulations in Figs. 9, 11, 13, and 15 related to the electro-hydraulic servomechanism, the behaviours of the two systems, made analogous through the choice of coefficients using formulas (4) – (8), are completely coincident.

- The mass-spring-damper system can simulate the behaviour of the electrohydraulic or electromechanical servomechanism quite effectively. However, it requires careful consideration when choosing coefficients to avoid potential errors.
- Employing simplified models to simulate significantly more complex systems is a powerful tool for accelerating simulations. It renders complex systems more manageable and comprehensible without delving into the analysis of their constituent subsystems.

The simplified models are also particularly useful in the development of real-time monitoring software for systems capable of operating in-flight, especially when the workload on on-board computers is particularly high.

As part of future work, there are plans to develop various simplified models, each assigned specific tasks to simulate diverse behaviours of aerospace electromechanical and electrohydraulic servomechanisms.

REFERENCES

[1] Parid Alimhillaj, Majlinda Alcani, Matteo D. L. Dalla Vedova, Luis Lamani, Spartak Pocari. Coulomb Friction Model Analysis, Acting on an Aerospace Servocommand. *Proceedings of the Joint International Conference: 10th Textile Conference and 4th Conference on Engineering and Entrepreneurship* 19-20 October, Tirana, Albania, Springer 2024, pp. 197-210.

[2] Dalla Vedova M.D.L. and Alimhillaj P., Numerical simulation of servovalves for electrohydraulic systems: a novel simplified fluid dynamic model sensitive to hydraulic capacity. *13th EASN International Conference on Innovation in Aviation & Space for opening New Horizons*, 05-08 September 2023, Salerno, Italy.

[3] Dorri A., Poçari S., Londo A. and Alimhillaj P., PID Control for Pneumatic Cylinder Stiffness for Aerospace Applications. *International Journal of Mechanics and Control*, Vol. 24, No. 01, 2023.

[4] Viersma T.J., *Analysis Synthesis and Design of Hydraulic Servo-systems and Pipelines*, Elsevier, Delft, 1980.

[5] Alimhillaj P., Poçari S. and Londo A., Software analysis comparison for the behavior of an aerospace servocommand in proportional control logic. *International Journal of Mechanics and Control*, Vol. 23, No. 01, pp. 77-82, 2022.

[6] Dalla Vedova M.D.L. and Alimhillaj P., Valve digital twins for electro-hydraulic actuator prognostics: snthetic fluid dynamic models sensitive to hydraulic capacity. *12th EASN, International Conference on Innovation in Aviation and Space for opening New Horizons*, 18-21 October 2022, Barcelona, Spain.

[7] Dalla Vedova M.D.L. and Alimhillaj P., Novel fluid dynamic nonlinear numerical models of servovalves for aerospace. *International Journal of Mechanics*, Vol. 13, 2019.

[8] Borello L. and Villero G., Confronto fra modelli semplificati di valvole di comando, *XI Congresso Nazionale A.I.D.A.A.,* Forlì, 14÷18 Ottobre 1991.

[9] Alimhillaj P. and Londo A., Modelisation of an Electromechanical Servomechanism for Aircraft Commands through MATLAB/SIMULINK. *National Bulletin of Technical Science*, Tirana, Albania, 2018.

[10] Jacazio G. and Borello L., A non-linear model of an electrohydraulic servo system with axial piston hydraulic motor. *7th International Fluid Power Symposium*, 16-18 September 1986, Bath-England.

[11] Quinn D.D., A new regularization of Coulomb friction. *ASME: Journal of Vibration and Acoustics,* Vol. 126, No. 3, pp. 391-397, 2004.

[12] Jacazio G. and Borello L., Mathematical models of electrohydraulic servovalves for fly-by-wire flight control systems. *6th Int. Congress on Mathematical Modelling*, August 1987, St. Louis-Missouri-U.S.A.

[13] Karnopp, D., Computer simulation of stick-slip in mechanical dynamic systems. *ASME Journal of Dynamic Systems, Measurement, and Control,* Vol. 107, No. 1, pp. 100-103, 1985.

[14] Dalla Vedova M.D.L., Berri P.C., Corsi C. and Alimhillaj P., New synthetic fluid dynamic model for aerospace four-ways servovalve. *International Journal of Mechanics and Control*, Vol. 20, No. 2, pp. 105-112, 2019.

52